IEEE Robotics and Automation Letters (RA-L) paper, presented at ICRA 2026, Vienna, Austria. Cite as RA-L paper.

A Human Finger-Inspired Rigid-Soft Hybrid Gripper for Damage-Free and Fast Grasping

Pengyu Zhou[1], Zeyang Gao[1], Xiaoxu Zhang[1,2,3], *Member IEEE*, Xiaowen Yin[1], Hongbin Fang[1,2,3], *Member IEEE* and Jian Xu[1]

***Abstract*—Rigid-soft hybrid grippers show good protection and high-payload capacity for fragile and heavy objects. However, because of inadequate actuation speed, it is still challenging for hybrid grippers to grasp moving objects in unstructured environments. To address this limitation, this article presents a rigid-soft hybrid gripper that can manually switch between four grasping modes, enabling it to not only grasp deformable and heavy objects like tofu and a dumbbell, but also capture moving objects with a low response time. Inspired by the structure of human fingers, a rigid-soft hybrid finger with a soft outer body and a rigid inner skeleton is designed. The finger consists of a soft pneumatic actuator (SPA), an endoskeleton linkage, a self-locking mechanism, a fast-responding mechanism, a pneumatic artificial muscle actuator (PAMA), a power transition bolt, and two split pins. The fast response speed of the PAMA and the amplification of the endoskeleton linkage enable the gripper to capture moving objects. A kinematic model is established to verify the endoskeleton linkage's angular velocity amplification ability and describe its bending angle. Experiments demonstrate that the rigid-soft finger can bend to 145.14° within 71 ms. Eventually, the gripper is mounted on a robotic arm to demonstrate that it can grasp fragile and deformable objects, hold heavy objects, and capture moving objects. The grasping strategies and structure of the gripper provide a new idea for designing a high-performance rigid-soft hybrid gripper.**

***Index Terms*—Low response time, multimode grasping, rigid-soft hybrid grippers, soft pneumatic actuators.**

I. Introduction

SOFT pneumatic grippers, with their low cost, simple structure, and ease of fabrication, have been widely used in pick-and-place tasks [1], [2], [3], [4]. Soft grippers provide excellent protection compared to rigid grippers, but their low load capacity remains a problem [5]. To improve the load capacity of soft grippers, researchers have developed various soft grippers, including those equipped with suction cups [6], employing dry adhesives [7], or using electro-adhesion [8]. However, these types of soft grippers have limitations when grasping deformable fragile objects like tofu, cake, and jelly. For instance, suction cups are only suitable for objects with rigid and smooth surfaces; dry adhesives require an additional preloading mechanism that may damage objects; and electro-adhesion requires high voltage that may break down soft materials. Therefore, soft pneumatic grippers using contact gripping show a unique advantage in grasping deformable fragile objects.

Variable stiffness materials and structures can enhance the full or local stiffness of soft pneumatic grippers to improve the load-bearing conditions to resist shape change. Therefore, these methods help improve the load capacity of soft pneumatic grippers. Variable stiffness materials like shape memory polymers (SMP) will change their Young's modulus by thermal field effect to alter stiffness [9], [10]. Thus, this method suffers from low response speed. On the other hand, variable stiffness structures can employ particle [11], fiber [12], and layer [13] [14] jamming structures to improve the stiffness of soft grippers. The increased static friction between elements will sharply enhance the stiffness of jamming structures when negative pressure is applied, which enhances the stiffness of soft grippers. Those methods have been demonstrated to improve the load capacity of soft grippers to 1.8, 1.46, 0.54, 0.5, 0.65, and 10 kg, respectively [9]-[14].

Rigid-soft hybrid grippers are another effective method, combining the high load capacity of rigid grippers with the protection capability of soft grippers. Guo et al. developed a soft-rigid gripper that uses a ratchet and a spring to improve the load capacity of a soft pneumatic gripper to 9 kg [15]. Utilizing a self-locking mechanism to improve the load capacity is a suitable method. Zhu et al. proposed a rigid-soft-coupled finger that can grasp 0.1 g potato chips to 27 kg dumbbells [16]. This design shows an excellent combination of soft and rigid actuators, respectively, driven by positive and negative pressure. In addition, a dual-modal hybrid gripper can adjust the contact stiffness between objects and the gripper by moving the rigid frame position, allowing it to catch 5.1 kg objects [17]. Wang et al. present a hybrid ratchet joint that can tune its locking torque by activating specific clutching ratchets, which achieve the rigid-soft hybrid gripper to lift a 4 kg dumbbell [18]. The above literature demonstrates that rigid-soft grippers collaborate with each other to inherit advantages. The maximum load capacity of the rigid-soft method is 2.7 times (27 kg/10 kg) that of the tunable stiffness

Manuscript received: April, 14, 2025; Revised July, 2, 2025; Accepted September, 1, 2025.

This paper was recommended for publication by Editor Yong-Lae Park upon evaluation of the Associate Editor and Reviewers' comments.

This work was supported by the National Natural Science Foundation of China (Grant No. 12372065, 12532002, U2441202) and the Shanghai Pilot Program for Basic Research-Fudan University (Grant No. 21TQ1400100-22TQ009). (Corresponding author: Xiaoxu Zhang)

[1]Pengyu Zhou, Zeyang Gao, Xiaoxu Zhang, Xiaowen Yin, Hongbin Fang, and Jian Xu are with College of Intelligent Robotics and Advanced Manufact uring, Fudan University, Shanghai, China (Email: 23110860024@m.fudan.ed u.cn; 23210860009@m.fudan.edu.cn; zhangxiaoxu@fudan.edu.cn; 21307140 083@m.fudan.edu.cn; fanghongbin@fudan.edu.cn; jian_xu@fudan.edu.cn)

[2]Xiaoxu Zhang and Hongbin Fang are with MOE Frontiers Center for Brain Science, Fudan University, Shanghai 200433, China (Email: zhangxiaoxu@fudan.edu.cn; fanghongbin@fudan.edu.cn).

[3]Xiaoxu Zhang and Hongbin Fang are with Yiwu Research Institute, Fudan University, Yiwu 322000, China. (Email: zhangxiaoxu@fudan.edu.cn; fanghongbin@fudan.edu.cn).

Digital Object Identifier (DOI): see top of this page.

©2026 IEEE

method. Selecting the rigid-soft method is expected to improve the load capacity of soft grippers significantly. However, these grippers do not consider moving objects, which requires a fast response speed of grippers.

Capturing moving targets remains challenging for humans and even more challenging for soft grippers. The ability to capture moving objects can extend the usable range of soft grippers to unstructured environments. For humans, capturing moving targets requires the coordination of eyes and hands. Soft grippers need to coordinate actuation and perception to grasp moving objects. Thus, this problem can be divided into actuation and perception. This paper focuses on the structure design of fast-response soft grippers. Zhang et al. developed a soft gripper employing two types of bistable mechanisms, realizing a response time of less than 200 ms [19]. Additionally, a flower-shaped gripper is made of bistable carbon composites, and its fastest response time for the snap-through process is 240 ms [20]. Utilizing a sudden change in the potential energy of bistable mechanisms and materials can remarkably reduce the response time of soft grippers. Furthermore, the response time of a vacuum-driven gripper is less than 320 ms [21]. Zhang et al. designed a rapid energy harvesting and dissipation mechanism for soft pneumatic grippers, which enables the gripper to capture high-speed targets within 30 ms [22]. It is noted that soft pneumatic actuation offers the advantages of diversity in structural design and material selection, enabling rapid response speeds [5], [23], [24]. However, complex pneu-net structures increase the response time, and their compliance poses a challenge to capturing moving objects stably. Therefore, combining rigid mechanisms can help soft pneumatic grippers improve response speed and increase the stability of capturing moving objects [25].

This paper presented a rigid-soft gripper that can grasp fragile, heavy, and moving objects. A rigid-soft finger consists of a soft pneumatic actuator (SPA), an endoskeleton linkage, a self-locking mechanism, a fast-responding mechanism, and a pneumatic artificial muscle actuator (PAMA). The gripper has four grasping modes to grasp light and fragile objects, deformable objects, heavy objects, and moving objects. Moreover, a kinematic model is established to verify the angular velocity amplification ability of the endoskeleton linkage and predict its bending angle. Experiments are conducted to describe the bending angle and output force of the SPA, the endoskeleton linkage, and rigid-soft finger. In addition, the proposed rigid-soft gripper can grasp deformable objects, including tofu and jelly, hook a 4.57 kg dumbbell, and capture a moving tennis ball. The main contributions of this article are summarized as follows.

1) A rigid-soft gripper with an SPA on the outside and an endoskeleton linkage on the inside is developed, taking inspiration from the structure of human hands. It can grasp deformable fragile objects up to 336.2 g.
2) Inspired by human grasping strategies, a self-locking mechanism is proposed to lock the finger in a bending state for hooking objects without continuous input.
3) Combining the fast response of pneumatic artificial muscle and the angular velocity amplification ability of the endoskeleton linkage, the rigid-soft finger can bend to 145.14° within 71 ms.

II. Design and Structure

The outside of a human finger is soft flesh and skin, and the inside is hard bone. Inspired by this, a rigid-soft hybrid finger is proposed in the paper, as shown in Fig. 1. The outside of the finger is SPA (the SPA is divided into two independent air chambers) to touch objects gently, and the endoskeleton linkage is sandwiched between two air chambers to provide enough grasping force. Fig. 1(a) and (b) show the rendered graph and rigid components of the finger, respectively. A rigid-soft finger consists of a SPA, an endoskeleton linkage (highlighted in grey), a self-locking mechanism (red), a fast-responding mechanism (purple), a PAMA, a power transition bolt, a split pin 1, and a split pin 2. The PAMA provides a linear motion to the self-locking mechanism or the fast-responding mechanism. Then, they transferred the power to the endoskeleton linkage. The two-finger rigid-soft gripper has four grasping modes when the endoskeleton linkage and SPA are activated independently or cooperatively. The power transition bolt, split pin 1, and split pin 2 are responsible for connecting the PAMA and endoskeleton linkage to the self-locking mechanism or fast-responding mechanism, enabling the gripper to switch between different grasping modes. Four grasping modes are switched manually and described as follows.

Mode 1: The self-locking mechanism and fast-responding mechanism are disconnected from the PAMA, and the input link-S connects to link 1 of the endoskeleton linkage by the power transition bolt (Fig. 1(c)). The gripper can grasp lightweight and fragile objects when the SPA is actuated individually, as shown in Fig. 2(a). The endoskeleton linkage will bend passively by the SPA.

Mode 2: With the weight of target objects increasing, the self-locking mechanism is set to connect the PAMA via split pin 2, while the input link-S still connects to link 1 via the power transition bolt (Fig. 1(d)). Green arrows indicate the process of power transmission from the PAMA. Inspired by the previous work, a safe grasping strategy is designed, as shown in Fig. 2(b) [26]. If the object is deformable and fragile, the SPA and endoskeleton linkage can be activated sequentially to realize safe grasping. The grasping process is similar to the strategy that humans use to grasp tofu. If the object is not susceptible to damage, the SPA and endoskeleton linkage can work simultaneously, or the endoskeleton linkage can work individually.

Mode 3: If the object is too heavy to hold in Mode 2, the finger can activate the self-locking function with the current connection state (Fig. 1(d)). Humans will fix four fingers and use the thumb to assist in holding heavy objects like a dumbbell, as shown in Fig. 2(c). A finger of the gripper bends and locks when the input pressure reaches the specific threshold value, and then another finger bends to assist in the

IEEE Robotics and Automation Letters (RA-L) paper, presented at ICRA 2026, Vienna, Austria. Cite as RA-L paper.

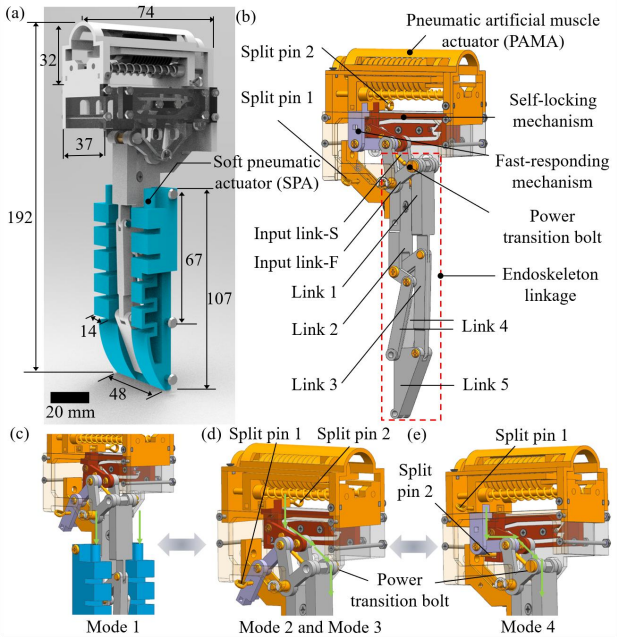

Fig. 1. Design of the rigid-soft hybrid finger. (a) The rendered graph of the rigid-soft hybrid finger. (b) The rigid components of the finger. (c) The connection of the self-locking mechanism, the fast-responding mechanism, and the endoskeleton linkage in Mode 1. (d) The connection of the PAMA, the self-locking mechanism, and the endoskeleton linkage in Modes 2 and 3. (e) The connection of the PAMA, the fast-responding mechanism, and the endoskeleton linkage in Mode 4.

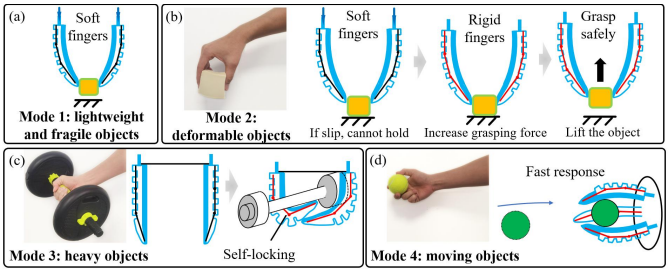

Fig. 2. Grasping strategies of the rigid-soft hybrid gripper. Grasping strategies of (a) grasping lightweight and fragile objects, (b) grasping deformable objects, (c) holding heavy objects, and (d) capturing moving objects.

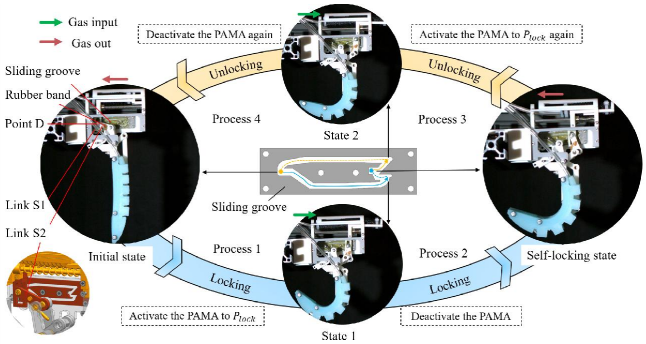

Fig. 3. Working process of the self-locking mechanism in Mode 3.

self-locking finger. The self-locking mechanism is designed to leverage the rigid mechanism's high load, enabling the finger to be locked in a specific location. Fig. 3 illustrates that the self-locking mechanism comprises four components: the sliding groove, a rubber band, link S1, and link S2. The working process of the self-locking mechanism is described as follows (Supplementary Video S1).

1): Activate the PAMA. Increasing the input pressure of the PAMA to P_{lock}, point D will move along the solid blue line and arrive at the arrow position in the sliding groove.

2): Deactivate the PAMA. After turning off the input pressure of the PAMA, Point D will reach the blue point along the blue dotted line under the action of the PAMA's springs. In this state, Point D is locked in this position of the sliding groove, enabling the finger to reach a self-locking state. Additionally, the finger can maintain its self-locking state without continuous input.

3): Activate the PAMA. To release the self-locking state, the PAMA increases the input pressure to P_{lock} again. Point D will move along the solid yellow line under the action of the PAM and arrive at the arrow position.

4): Deactivate the PAMA. After turning off the PAMA, it returns to its original position (yellow point) of the sliding groove along the yellow dotted line under the action of springs.

The rubber band is added to ensure that Point D returns to its original position, which guarantees that Point D will move along the same path in subsequent activations.

Mode 4: The fast-responding mechanism is set to connect the endoskeleton linkage and PAMA by split pin 1, and the input link-F connects to link 1 by the power transition bolt (Fig. 1(e)). As shown in Fig. 2(d), reducing the response time and increasing the grasping stability for the gripper are crucial for capturing moving objects. The PAMA has a low response time and a large output force. Additionally, the endoskeleton linkage is designed to improve the response speed of the fingertip compared to that of the input. Therefore, the rigid-soft gripper has the potential to capture moving objects.

PAMs have the advantages of significant elongation, large output force, and low response time, allowing them to be employed in soft robot design [27], [28]. The PAMA in this paper is made of a 55-mm length, 7-mm external diameter, and 2-mm thickness silicone rubber tube. Fig. 4 shows the prototype and performance of the PAMA. When the gas is input into the PAM, the PAM elongates, realizing that part 4 moves along the cylindrical pins. After turning off the input, two springs help the PAM and Part 4 recover to the initial position. The PAMA's maximal displacement and force are 38.34 mm and 16.22 N, respectively, with the 300 kPa input pressure. Additionally, its actuating time is 90 ms under 300 kPa. The performance tests have shown that the movement range and response time of the PAMA can meet the design requirements.

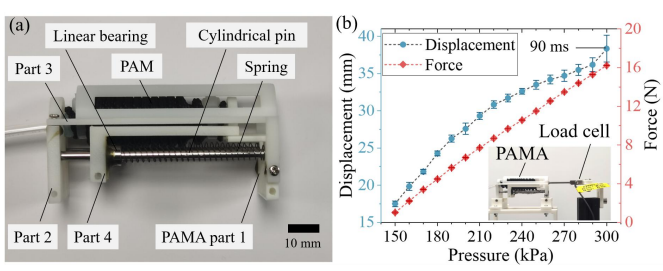

Fig. 4. (a) The prototype of the PAMA. (b) Performance of the PAMA.

IEEE Robotics and Automation Letters (RA-L) paper, presented at ICRA 2026, Vienna, Austria. Cite as RA-L paper.

III. Theoretical Model

The rigid-soft finger developed in this paper has the advantages of a large bending angle range and fast response speed. The endoskeleton linkage can be regarded as a rigid actuator that plays an important role in enhancing SPA performance. Therefore, this part introduces a kinematic model to verify the angular velocity amplification ability of the endoskeleton linkage. In addition, the kinematic model can describe the relationship between the input angle and the fingertip's bending angle.

The kinematic model of endoskeleton linkage is established by the vector loop method, and Fig. 5(a) and Table I show the design parameters of the endoskeleton linkage. Because of the symmetry of the structure, input link-S and input link-F are called input links here, and the input angle of the endoskeleton linkage is the rotation angle of link 2 $\alpha_{in,2}$. First, the coordinate origin O is set on the rotating shaft of the input link. Second, vectors are assigned to each link. The positive x-axis is defined to 0°, and clockwise rotation angle between the link and the positive x-axis is defined as positive. Third, four vector looped equations can be written as follows:

$$\boldsymbol{r}_{in,2} + \boldsymbol{r}_1 - \boldsymbol{r}_{3,1} - \boldsymbol{r}_{2,1} = \boldsymbol{0} \quad (1)$$

$$\boldsymbol{r}_{3,1} + \boldsymbol{r}_{3,2} - \boldsymbol{r}_{5,1} - \boldsymbol{r}_4 - \boldsymbol{r}_{2,2} = \boldsymbol{0} \quad (2)$$

$$\boldsymbol{r}_{3,1} + \boldsymbol{r}_{3,2} - \boldsymbol{r}_{3,3} = \boldsymbol{0} \quad (3)$$

$$\boldsymbol{r}_{5,1} - \boldsymbol{r}_{5,2} + \boldsymbol{r}_{5,3} = \boldsymbol{0} \quad (4)$$

where $\boldsymbol{r}_{in,2}$, $\boldsymbol{r}_1$, $\boldsymbol{r}_{2,1}$, $\boldsymbol{r}_{2,2}$, $\boldsymbol{r}_{3,1}$, $\boldsymbol{r}_{3,2}$, $\boldsymbol{r}_{3,3}$, $\boldsymbol{r}_4$, $\boldsymbol{r}_{5,1}$, $\boldsymbol{r}_{5,2}$, and $\boldsymbol{r}_{5,3}$ correspond to input link 2, link-1, link 2-1, link 2-2, link 3-1, link 3-2, link 3-3, link 4, link 5-1, link 5-2, and link 5-3, respectively. Each vector is mathematically described by the length, the initial angle, and the rotation angle of its corresponding link. Lengths and initial angles of links are shown in Table I. Then four equations are resolved into x-axis and y-axis components, so we get eight equations. As shown in Fig. 5(b), the bending angle θ of the fingertip is defined as the angle between link 5-2 and the negative y-axis. Furthermore, the bending angle θ is equal to the rotation angle $\alpha_{5,2}$ of link 5-2, meaning that $\theta = \alpha_{5,2}$. The rotation angle $\alpha_{5,2}$ can be solved by eight equations derived from equations (1)-(4). Therefore, the bending angle of fingertip θ can be obtained. It is assumed that the input link 2 bends with a constant speed. The fingertip's rotation angle is larger than the input's rotation angle taking the same amount of time. Thus, the angular velocity amplification ratio R is defined as the ratio of the fingertip's rotation angle to the input's rotation angle:

$$R = \frac{\alpha_{5,2}}{\alpha_{in,2}} \quad (5)$$

where $\alpha_{5,2}$ and $\alpha_{in,2}$ are the rotation angle of the fingertip and input link, respectively.

IV. Experiment and Discussion

In this Section, the SPA, the endoskeleton linkage, and the rigid-soft finger's bending angle and tip force are measured. In addition, the rigid-soft gripper is demonstrated to have the advantages of protecting deformable objects, holding heavy objects, and having low response time to moving objects. Eventually, the rigid-soft gripper is mounted on a robotic arm to grasp fragile and deformable objects, hold heavy objects, and capture moving objects.

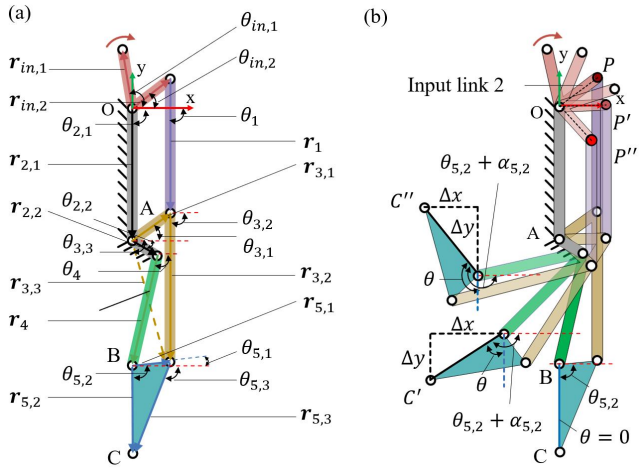

Fig. 5. Schematic diagrams for modeling the endoskeleton linkage. (a) Parameters of the endoskeleton linkage. (b) Motion schematic diagram of the endoskeleton linkage.

Table I
The Design Parameters of the Endoskeleton Linkage

Link	Vector	Length (mm)	Initial angle (°)	Rotation angle
Input link	$\boldsymbol{r}_{in,1}$	$l_{in,1}$: 20	$\theta_{in,1}$: -99.47	$\alpha_{in,1}$
	$\boldsymbol{r}_{in,2}$	$l_{in,2}$: 15.5	$\theta_{in,2}$: -34.47	$\alpha_{in,2}$
Link 1	$\boldsymbol{r}_1$	l_1: 45	θ_1: 89.43	α_1
Link 2	$\boldsymbol{r}_{2,1}$	$l_{2,1}$: 45	$\theta_{2,1}$: 90	0
	$\boldsymbol{r}_{2,2}$	$l_{2,1}$: 10	$\theta_{2,2}$: 30	0
Link 3	$\boldsymbol{r}_{3,1}$	$l_{3,1}$: 15.87	$\theta_{3,1}$: -33.57	$\alpha_{3,1}$
	$\boldsymbol{r}_{3,2}$	$l_{3,2}$: 50	$\theta_{3,2}$: 91.43	$\alpha_{3,2}$
	$\boldsymbol{r}_{3,3}$	$l_{3,3}$: 42.91	$\theta_{3,3}$: 73.80	$\alpha_{3,3}$
Link 4	$\boldsymbol{r}_4$	l_4: 38	θ_4: 103.17	α_4
Link 5	$\boldsymbol{r}_{5,1}$	$l_{5,1}$: 12	$\theta_{5,1}$: -3.78	$\alpha_{5,1}$
	$\boldsymbol{r}_{5,2}$	$l_{5,2}$: 30	$\theta_{5,2}$: 90	$\alpha_{5,2}$
	$\boldsymbol{r}_{5,3}$	$l_{5,3}$: 33.04	$\theta_{5,3}$: 112.12	$\alpha_{5,3}$

A. Performance of the Rigid-Soft Hybrid Finger

A finger is composed of a SPA, an endoskeleton linkage, a self-locking mechanism, a fast-responding mechanism, and a PAMA. The SPA and the silicone tube of PAMA are cast in commercial soft and stretchable rubber (Dragon Skin 30, Smooth-on Inc.). The links and structural frames are manufactured by 3-D printing. Fig. 6 exhibits the experimental platform, and the SPA, the endoskeleton linkage, and the finger are mounted on an aluminous support to measure the bending angle and tip force. A high-speed camera (Phantom VEO E340L, Vision Research Inc.) captures the movement to measure the bending angle, and a load cell measures the tip force. Other experimental facilities are proportional valves (ITV2031-312L, SMC), solenoid valves, a power supply, DC powers, and switches.

Experimental results are shown in Fig. 7, and Fig. 7(a) shows that the bending angle and tip force of the SPA increase

IEEE Robotics and Automation Letters (RA-L) paper, presented at ICRA 2026, Vienna, Austria. Cite as RA-L paper.

monotonically with increasing input pressure. When it naturally droops due to gravity, the SPA's fingertip angle is 4.11°. The SPA realizes a relatively large bending angle range thanks to the design of the large chamber gap. Fig. 7(b) shows the bending angle and force of the endoskeleton linkage actuated by the PAMA. The bending angle curves of the kinematic model and experimental data have a satisfactory degree of fitting, with a Pearson correlation coefficient of 0.99. The endoskeleton linkage reaches a locked state when the input pressure increases to 290 kPa. It is noted that the self-locking pressure P_{lock} will increase to 320 kPa when the SPA is assembled into the endoskeleton linkage.

Fig. 7(c) and (d) show the bending angle and tip force with combined actuation of SPA and endoskeleton linkage (driven by PAMA). In addition, the maximal bending angle and force of the SPA, the endoskeleton linkage, and the finger are listed in Table II. The SPA's maximum bending angle and tip force are 72.09 ° and 0.618 N, respectively. The endoskeleton linkage's bending angle and force are 82.31 ° and 0.654 N, respectively, when the initial input of the PAMA is 150 kPa, which shows that the endoskeleton linkage can make up for SPA's lack of grasping force. The maximal bending angle of the endoskeleton linkage is 145.69°. However, the maximal bending angle of the rigid-soft finger decreases to 140.6 °, which is caused by the resistance of the SPA.

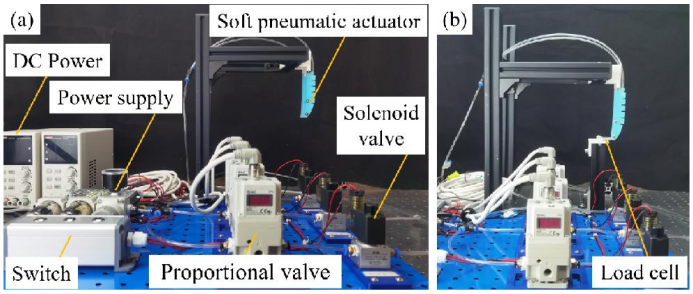

Fig. 6. The experimental platform for measuring (a) the bending angle and (b) tip force of the SPA, endoskeleton linkage, and the rigid-soft finger.

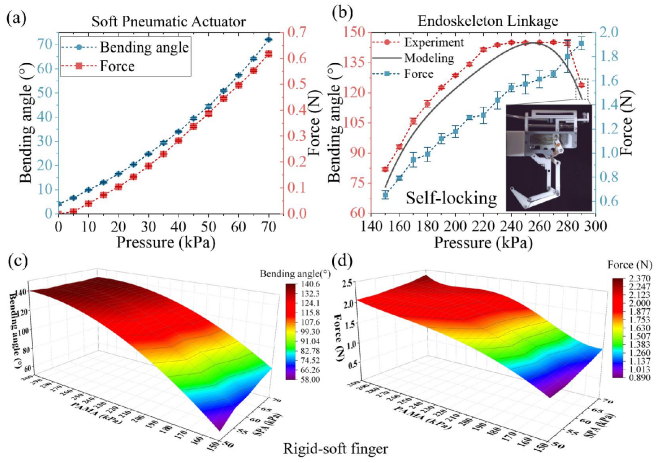

Fig. 7. Performance of the SPA, the endoskeleton linkage, and the rigid-soft finger (a) Input pressure vs. bending angle and force of SPA. (b) Input pressure vs. bending angle and force of endoskeleton linkage. (c) Relationship between the input pressure and the bending angle of the finger. (d) Relationship between the input pressure and the tip force of the finger.

Table II
THE PERFORMANCE OF THE SPA, THE ENDOSKELETON LINKAGE, AND THE FINGER

	Bending angle (°)	Force (N)
Soft pneumatic actuator	72.09	0.618
Endoskeleton linkage	145.69	1.911
Rigid-soft finger	140.60	2.370

B. Verification of Damage-Free Grasping

As shown in Fig. 8, a two-finger rigid-soft hybrid gripper grasps a deformable plastic cup and a balloon to verify its ability to engage in damage-free grasping. The gripper turns to Mode 2, and the self-locking mechanism connects the endoskeleton linkage and PAMA. First, the gripper can readily grasp a plastic cup at 60 kPa of the SPA. Then a 100 g and a 200 g weight are put into the cup. The gripper can grasp the plastic cup stably by activating the PAMA with 150 kPa and 200 kPa, respectively, and the cup deforms slightly. It is proved that the external soft material and the sliding groove of the self-locking mechanism reduce the impact on objects. The previous work has shown that a soft pneumatic gripper made of common soft materials grasps a plastic cup with a 100 g weight; the cup will deform seriously due to the impact produced by the soft actuator [26]. Furthermore, a 1.5 g balloon filled with air can be held by actuating SPA at 30 kPa, while a 144.3 g balloon filled with water requires PAMA actuation at 160 kPa. To grasp a 336.2 g balloon with water, the rigid-soft gripper activates the SPA and PAMA at 60 kPa and 200 kPa sequentially. The balloon is held gently and stably. Thus, the experiment results have proved that the rigid-soft gripper can grasp deformable objects.

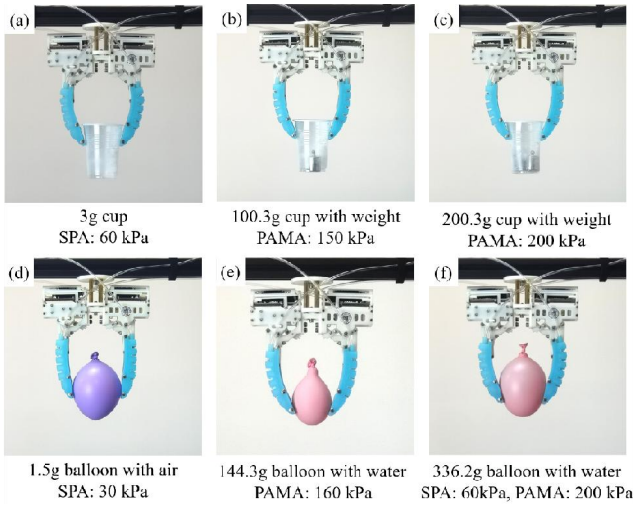

Fig. 8. Validation of grasping deformable objects. The rigid-soft gripper safely grasps (a) a 3 g cup, (b) a 100.3 g cup with weight, (c) a 100.3 g cup with weight, (d) a 1.5 g balloon with air, (e) a 144.3 g balloon with water, and (f) a 336.2 g balloon with water.

C. Evaluation of the Load Capacity

Experiments are conducted to evaluate the load capacity of the rigid-soft hybrid gripper when activating the self-locking mechanism of the finger. Fig. 9 shows that the single-finger,

two-finger, and three-finger grippers hold a 2.29 kg basket, a 3.34 kg dumbbell, and a 4.57 kg dumbbell steadily. The fingers of the single-finger and the three-finger gripper are all in the self-locking state, and the two-finger gripper holds the dumbbell in Mode 3. The weight of the single-finger, two-finger gripper, and three-finger gripper, including air tubes, are 170.9 g, 365 g, and 609.3 g, respectively. Thus, they achieve a 13.4, 9.2, and 7.5 payload-to-weight ratio. The 13.4 payload-to-weight ratio falls within a medium range compared to 24 soft-rigid grippers [25]. The rigid mechanism can use materials with a better Young's modulus to further improve the load capacity in the future.

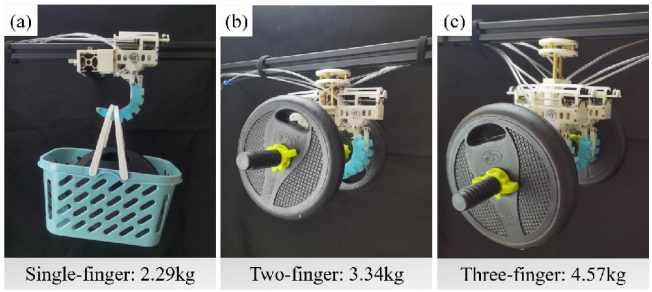

Fig. 9. Validation of grasping heavy objects. (a) Single finger holds a 2.29 kg basket. (b) Two-finger rigid-soft gripper holds a 3.34 kg dumbbell. (c) Three-finger rigid-soft gripper holds a 4.57 kg dumbbell.

D. Verification of the Fast Grasping

Fig. 10(a) shows the angular velocity amplification ratio of the fingertip and the input from experimental data and theoretical model. The prototype's bending angle ratios are measured with different input pressures of the PAMA. The ratios of the model and experimental data are 1.77-1.80 and 1.67-1.78, respectively. The accuracy is from 93% to 100%, and the RMSE is 0.057. The model error is that the model is calculated under ideal conditions without considering joint looseness. In general, the theoretical model is close to the experimental data, which verifies that the endoskeleton linkage can improve the response speed of the input.

The response time of the finger is measured first to evaluate whether the rigid-soft hybrid gripper can be used to grasp moving objects. The finger's movement is captured by a high-speed camera with 800 FPS. The response time and bending angle of the SPA and the rigid-soft hybrid finger in different input conditions are shown in Fig. 10(b). The first item of the bar graph is the experimental result of the SPA, and the following three items are those of the rigid-soft hybrid finger. The response time of SPA is measured from the stationary state to the moment when motion begins (as the initial frame) to the moment when the maximum bending angle is just reached (as the end frame). Because the SPA will vibrate after reaching the maximum bending angle. It is observed that the SPA takes 177.5 ms from static state to 88.67 ° (Supplementary Video S2). The finger can bend to 145.14 ° within 71 ms with 300 kPa input pressure of the PAMA. The response time has decreased by 60%, and the bending range has increased by 63.7%. Note that the finger bends to 147.95° within 74.75 ms with 60 kPa and 300 kPa input pressure of SPA and the PAMA together. The experimental results show that the average response time of cooperative input for SPA and PAMA is more than that of the individual PAMA input. Actually, the best test results can be reduced to 61.25 ms when the SPA and PAMA are triggered simultaneously. The inconsistency in trigger time causes this because the SPA and PAMA are triggered by manually pressing the buttons, leading to a large measurement error. On the other hand, the bending angle range increases from 145.14° to 147.95° when activating the SPA and the PAMA simultaneously. The reason is that the curving SPA does not restrict the motion of endoskeleton linkage, which naturally results in a large bending angle. In summary, the response time and bending angle in the two cases are not much different and can be regarded as the same order of magnitude. Therefore, the finger can activate the PAMA individually when it is used to capture moving objects.

With such a fast response speed, the two-finger and three-finger rigid-soft hybrid gripper tries to grasp moving objects. An object is thrown upwards, and the gripper is triggered and catches the object when the object reaches the end of the finger. As shown in Fig. 10(c)-(f), the two-finger gripper successfully grasps a moving tennis ball, a bag, a box, and a bottle within 120, 113, 281, and 215 ms, respectively. The response time is measured from the moment the object reaches the end of the finger (red line in Fig. 10) to the moment when the object is caught stably. In addition, the three-finger gripper can successfully capture a moving tennis ball, a bag, a box, and a bottle within 344, 238, 153, and 211 ms, respectively, as shown in Fig. 10(g)-(j) (Supplementary Video S3). Furthermore, Table III compares eight soft gripers with low response times. Although the response time in this paper is not the fastest, it is still competitive. Even if several literatures do not list the bending angle of their designed finger or gripper, the rigid-soft finger developed in this paper shows excellent performance with a relatively low response time and large bending range. The rigid-soft coupling method provides a new idea for improving response speed of pneumatic soft grippers.

Table III
COMPARISON OF FAST GRASPING SOFT GRIPPERS

Type	Response time (ms)	Bending angle (°)	Activation pattern
Tendon actuated bistable mechanism gripper [19]	200	50	Active
Pneumatically actuated bistable composited gripper [20]	240	-	Active
Vacuum driven bistable gripper [29]	180	-	Passive and active
Negative pressure actuated gripper [30]	100	~54	Passive and active
Vacuum driven gripper [21]	320	100	Active
Pneumatic energy harvesting and dissipation gripper [22]	34	-	Passive
Electrohydraulic driven gripper [31]	50	-	Active
Pneumatic rigid-soft hybrid gripper (This work)	71	145.14	Active

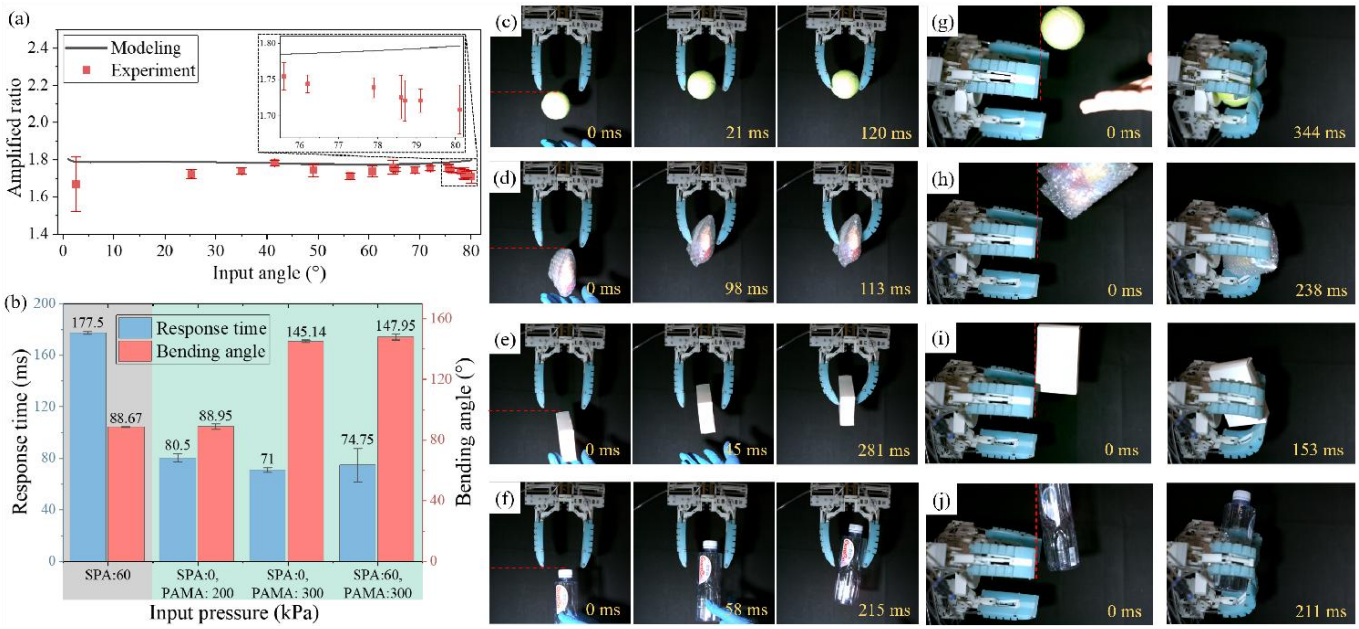

Fig. 10. Validation of grasping moving objects. (a) Comparison of angular velocity amplification ratios from experimental data and theoretical model. (b) Response time of the SPA and the rigid-soft finger with different pressure conditions. The two-finger rigid-soft gripper captures (c) a moving tennis ball, (d) a bag, (e) a box, and (f) a bottle. The three-finger rigid-soft gripper captures (g) a moving tennis ball, (h) a bag, (i) a box, and (j) a bottle.

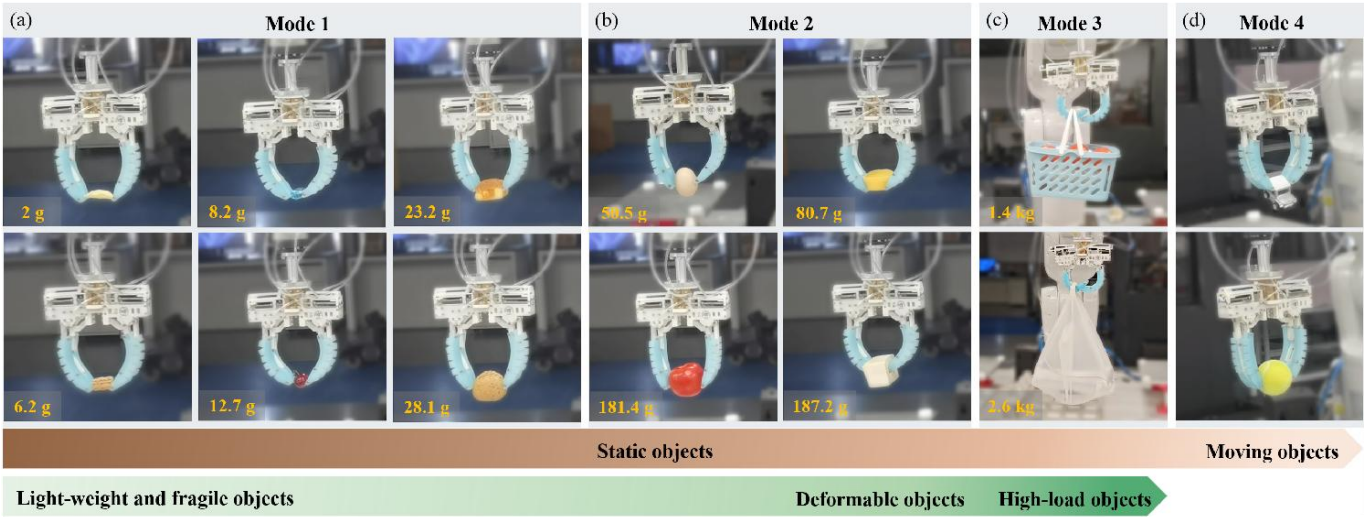

Fig. 11. The exhibition of grasping different types of objects. (a) The two-finger rigid-soft gripper pinches a 2 g chip, 6.2 g wafer biscuit, 8.2 g laundry ball, 12.7 g cherry, 23.2 g cake, and 28.1 g mochi in mode one. (b) The two-finger gripper grasps a 50.5 egg, 181.4 g tomato, 80.7 g jelly, and 187.2 g tofu in mode two. (c) The two-finger gripper holds a 1.4 kg basket and 2.6 kg plastic bag in mode three. (d) The two-finger gripper captures a moving toy car and a tennis ball.

E. Demonstration of Grasping Deformable, Heavy, and Moving Objects

The two-finger rigid-soft hybrid gripper is mounted to the robotic arm to grasp deformable, heavy, and moving objects, as shown in Fig. 11. The grasping processes are also demonstrated in the supplementary Video S4. When dealing with light and fragile objects, such as a 2 g chip, 6.2 g wafer biscuit, 8.2 g laundry ball, 12.7 g cherry, 23.2 g cake, and 28.1 g mochi, the gripper can pinch gently by activating the SPA individually in Mode 1. When the weight of objects increases, such as a 50.5 egg or 181.4 g tomato, the gripper can grasp by activating the PAMA individually in Mode 2. However, if surfaces of objects are deformable, such as an 80.7 jelly and 187.2 g tofu, the gripper can activate the SPA and the PAMA sequentially. Furthermore, the gripper can hook a 1.4 kg basket and 2.6 kg plastic bag using the self-locking mechanism in Mode 3. Eventually, the gripper captures a moving toy car and a tennis ball in Mode 4. The experiments demonstrate that the proposed rigid-soft gripper can effectively deal with deformable, heavy, and moving objects.

V. Conclusion

This article proposes a rigid-soft hybrid gripper that can grasp fragile, heavy, and moving objects. Inspired by the human finger's hybrid structure, a finger with a soft outer body and a rigid inner skeleton is developed, and the rigid-soft

finger consists of a SPA, an endoskeleton linkage, a self-locking mechanism, a fast-responding mechanism, a PAMA, a power transition bolt, and two split pins. Four grasping modes are designed for the two-finger gripper to grasp lightweight, fragile, deformable, heavy, and moving objects. A kinematic model is established to describe the endoskeleton linkage's bending angle and verify the angular velocity amplification ratio. Experiments describe the bending angle and tip force of the SPA, the endoskeleton linkage, and the rigid-soft hybrid finger and verify the accuracy of the theoretical model. The damage-free and fast grasping capacity of the gripper are validated, respectively. Eventually, the two-finger gripper is mounted on a robotic arm to demonstrate that it has the potential to grasp fragile and deformable objects, hold heavy objects, and capture moving objects. The grasping strategies and structure design proposed in this paper provide a new idea for designing a high-performance rigid-soft hybrid gripper.

Future work will focus on the finger's proprioceptive ability to identify the characteristics of target objects, including their size and weight. Moreover, the gripper's structure will be improved to realize automatic switching mode and grasping.

REFERENCES

[1] F. Ilievski, A. D. Mazzeo, R. F. Shepherd, X. Chen, and G. M. Whitesides, "Soft robotics for chemists," *Angew. Chem.*, vol. 123, no. 8, pp. 1930-1935, Feb. 2011.

[2] W. Kim et al., "Bioinspired dual-morphing stretchable origami," *Sci. Robot.*, vol. 4, no. 36, 2019, Art. no. eaay3493.

[3] Q. Guan, J. Sun, Y. Liu, N. M. Wereley, and J. Leng, "Novel bending and helical extensile/contractile pneumatic artificial muscles inspired by elephant trunk," *Soft Robot.*, vol. 7, no. 5, pp. 597-614, Oct. 2020.

[4] Z. Zhang, Y. Long, G. Chen, Q. Wu, H. Wang, and H. Jiang, "Soft and lightweight fabric enables powerful and high-range pneumatic actuation," *Sci. Adv.*, vol. 9, no. 15, 2023, Art. no. eadg1203.

[5] J. Shintake, V. Cacucciolo, D. Floreano, and H. Shea, "Soft robotic grippers," *Adv. Mater.*, vol. 30, no. 29, 2018, Art. no. 1707035.

[6] Z. Xie et al., "Octopus arm-inspired tapered soft actuators with suckers for improved grasping," *Soft Robot.*, vol. 7, no. 5, pp. 639-648, Oct. 2020.

[7] E. W. Hawkes, D. L. Christensen, Amy Kyungwon Han, H. Jiang, and M. R. Cutkosky, "Grasping without squeezing: shear adhesion gripper with fibrillar thin film," in *Proc. IEEE Int. Conf. Robot. Automat.*, May 2015, pp. 2305-2312.

[8] J. Shintake, S. Rosset, B. Schubert, D. Floreano, and H. Shea, "Versatile soft grippers with intrinsic electroadhesion based on multifunctional polymer actuators," *Adv. Mater.*, vol. 28, no. 2, pp. 231-238, Jan. 2016.

[9] T. T. Hoang, P. T. Phan, M. T. Thai, N. H. Lovell, and T. N. Do, "Bio-inspired conformable and helical soft fabric gripper with variable stiffness and touch sensing," *Adv. Mater. Technol.*, vol. 5, no. 12, 2020, Art. no. 2000724.

[10] J. Yan, Z. Xu, P. Shi, and J. Zhao, "A human-inspired soft finger with dual-mode morphing enabled by variable stiffness mechanism," *Soft Robot.*, vol. 9, no. 2, pp. 399-411, Apr. 2022.

[11] Y. Yang, Y. Zhang, Z. Kan, J. Zeng, and M. Y. Wang, "Hybrid jamming for bioinspired soft robotic fingers," *Soft Robot.*, vol. 7, no. 3, pp. 292-308, Jun. 2020.

[12] S. Jadhav, M. R. A. Majit, B. Shih, J. P. Schulze, and M. T. Tolley, "Variable stiffness devices using fiber jamming for application in soft robotics and wearable haptics," *Soft Robot.*, vol. 9, no. 1, pp. 173-186, Feb. 2022.

[13] W. Yu, J. Liu, X. Li, Z. Yu, and H. Yuan, "A novel hybrid variable stiffness mechanism: synergistic integration of layer jamming and shape memory polymer," *IEEE Robot. Autom. Lett.*, vol. 9, no. 3, pp. 2734-2741, Mar. 2024.

[14] J. Huang et al., "Autologous variable stiffness soft finger based on cross-layer jamming for multimode grasping," *IEEE Robot. Autom. Lett.*, vol. 10, no. 2, pp. 1178-1185, Feb. 2025.

[15] X. Guo, W. Li, Q. Gao, H. Yan, Y. Fei, and W. Zhang, "Self-locking mechanism for variable stiffness rigid-soft gripper," *Smart Mater. Struct.*, vol. 29, no. 3, 2020, Art. no. 035033.

[16] J. Zhu et al., "Bioinspired multimodal multipose hybrid fingers for wide-range force, compliant, and stable grasping," *Soft Robot.*, vol. 10, no. 1, pp. 30-39, Feb. 2023.

[17] J. Zhu, H. Chen, Z. Chai, H. Ding, and Z. Wu, "A dual-modal hybrid gripper with wide tunable contact stiffness range and high compliance for adaptive and wide-range grasping objects with diverse fragilities," *Soft Robot.*, vol. 11, no. 3, pp. 371-381, Jun. 2024.

[18] X. Wang and Q. Xu, "Design and development of a new bioinspired hybrid robotic gripper for multi-mode robust grasping," *IEEE Trans. Autom. Sci. Eng.*, vol. 21, no. 4, pp. 5473-5489, Oct. 2024.

[19] P. Zhang and B. Tang, "A two-finger soft gripper based on bistable mechanism," *IEEE Robot. Autom. Lett.*, vol. 7, no. 4, pp. 11330-11337, Oct. 2022.

[20] Z. Zhang et al., "Pneumatically controlled reconfigurable bistable bionic flower for robotic gripper," *Soft Robot.*, vol. 9, no. 4, pp. 657-668, Aug. 2022.

[21] Y. Long et al., "Lightweight and powerful vacuum-driven gripper with bioinspired elastic spine," *IEEE Robot. Autom. Lett.*, vol. 8, no. 12, pp. 8136-8143, Dec. 2023.

[22] Y. Zhang, W. Zhang, P. Gao, X. Zhong, and W. Pu, "Finger-palm synergistic soft gripper for dynamic capture via energy harvesting and dissipation," *Nat. Commun.*, vol. 13, no. 1, 2022, Art. no. 7700.

[23] N. El-Atab et al., "Soft actuators for soft robotic applications: A review," *Adv. Intell. Sys.*, vol. 2, no.10, 2020, Art. no. 2000128.

[24] M. S. Xavier et al., "Soft pneumatic actuators: A review of design, fabrication, modeling, sensing, control and applications," *IEEE Access*, vol. 10, pp. 59442-59485, Jun. 2022.

[25] L. Li et al., "A Comparative Analysis and Scoping Review of Soft–Rigid and Industrial Parallel Rigid Grippers," *Adv. Intell. Sys.*, vol. 7, no. 5, 2025, Art no. 2400503.

[26] X. Yin, P. Zhou, J. Xie, S. Tang, S. Wen, J. Zhang, and J. Li, "A human finger-inspired shape-locking pneumatic gripper enabled by folding laminar jamming structure," *IEEE/ASME Trans. Mechatron.*, vol. 29, no. 5, pp. 3626-3637, Oct. 2024.

[27] W. Wang et al., "A modular soft pipe-climbing robot with high maneuverability," *IEEE/ASME Trans. Mechatron.*, vol. 29, no. 6, pp. 4734-4743, Dec. 2024.

[28] W. Wang, Y. Zhu, S. Cai, and G. Bao, "Ultralong stretchable soft actuator (us2a): design, modeling and application," *Chin. J. Mech. Eng.*, vol. 36, no. 1, 2023, Art. no. 13.

[29] Y. Jiang et al., "Reprogrammable bistable actuators for multimodal, fast, and ultrasensitive grasping," *IEEE/ASME Trans. Mechatron.*, vol. 29, no. 2, pp. 984-994, Apr. 2024.

[30] Y. Lin et al., "A bioinspired stress-response strategy for high-speed soft grippers," *Adv. Sci.*, vol. 8, no. 21, 2021, Art. no. 2102539.

[31] Z. Yoder, D. Macari, G. Kleinwaks, I. Schmidt, E. Acome, and C. Keplinger, "A soft, fast and versatile electrohydraulic gripper with capacitive object size detection," *Adv. Funct. Mater.*, vol. 33, no. 3, 2023, Art. no. 2209080.